Emergency Management
Science and Technology

ARTICLE

Open Access

https://doi.org/10.48130/emst-0026-0005
Emergency Management Science and Technology **2026**, 6: e005

A data-driven decision support framework for emergency resource management in critical infrastructure

Amirhossein Yousefi Joobeni and Reza Dashti*

School of Advanced Technologies, Iran University of Science & Technology, Tehran 16-846-13114, Iran
* Correspondence: rdashti@iust.ac.ir (Dashti R)

Abstract

Effective emergency management of critical infrastructure following high-impact–low-probability events is a significant scientific and technological challenge. A critical failure point is often the lack of pre-positioned spare assets, which cripples recovery efforts. This paper proposes a data-driven decision-support framework to enhance emergency logistics and resource allocation. By integrating engineering fragility curves with a unique 10-year operational dataset, our model quantifies the precise number of asset failures required to ensure the rapid restoration of services. Specifically, we utilize historical failure records and meteorological data to calibrate asset fragility curves, moving beyond qualitative assessments. This framework enables emergency managers to shift from heuristic risk assessments to a data-driven budgeting process, quantifying inventory requirements to balance costs against the socioeconomic impact of prolonged disruptions. Our results provide a powerful scientific tool for enhancing the resilience and recovery capabilities of critical infrastructure systems.

Citation: Yousefi Joobeni A, Dashti R. 2026. A data-driven decision support framework for emergency resource management in critical infrastructure. *Emergency Management Science and Technology* 6: e005 https://doi.org/10.48130/emst-0026-0005

Introduction

Providing reliable electricity to meet society's needs is a major concern for countries globally. However, aging infrastructure and the increasing frequency of natural disasters pose significant threats to the stability of power systems. The electricity crisis in Pakistan serves as a prominent example of how supply deficits and vulnerabilities in the power grid can escalate into major political and socioeconomic issues[1]. Consequently, reliable assessment of the resilience of energy infrastructure to natural disasters is a paramount concern for researchers, government officials, and community members.

Resilience refers to the ability of a system to withstand, adapt to, and rapidly recover from disruptive events. Recent studies have established comprehensive frameworks for resilience-based infrastructure planning, particularly in the context of water distribution systems and urban sustainability[2]. Though metrics for resilience are evolving, the sensitivity of electric power infrastructure to the spatial distribution of disaster impacts creates significant uncertainty in recovery predictions[3]. Furthermore, given the high interdependency of critical infrastructure, joint restoration modeling has become essential for realistic resilience assessments[4]. These assessments are critical under extreme weather conditions, such as typhoons, where regulatory and operational frameworks are tested to their limits[5].

To enhance resilience, researchers have proposed various enhancement strategies. These range from robust optimization-based planning that incorporates distributed generation to mitigate the impact of natural disasters[6,7] through to dynamic operational strategies and mobile energy storage systems[8]. Strengthening the infrastructure against specific hazards remains a primary strategy, with studies quantifying the benefits of vegetation management and reinforcement strategies[9]. Insights from other critical infrastructure, such as telecommunications, further highlight the importance of post-disaster site surveys and the fragility of power plants during events like Hurricane Katrina[10]. Additionally, utility outage statistics have been utilized to quantify improvements in bulk power systems' resilience, emphasizing the need for data-driven approaches[11].

A key component of operational resilience is asset management. Effective management of asset performance within power grids is crucial for maintaining service quality[12]. This involves trade-offs between costs and reliability, such as the decision to invest in underground versus overhead lines[13]. Integrating risk analyses with multi-criteria decision support is a common approach in electricity distribution system-related asset management to prioritize investments[14]. Previous studies have also explored asset management models for specific equipment, such as public lighting systems, to evaluate economic performance[15]. Furthermore, recent research has highlighted the economic sustainability of asset management, analyzing the stability of repair activities and the impact of load growth and inflation on long-term planning in metropolitan grids[16].

Despite these advancements in resilience planning and economic asset management, a significant void remains in the quantitative modeling of pre-disaster warehousing for crisis scenarios. Most existing asset management models focus on steady-state reliability or long-term lifecycle costs. However, during high-impact–low-probability (HILP) events, the simultaneous failure of assets creates an immediate, massive demand for spare parts that conventional reliability models fail to predict. There is a lack of a practical, data-driven framework that directly integrates engineering fragility curves with real-world asset lifecycle data to optimize crisis inventories. Although economic models address the stability of routine repairs[17], they do not quantify the precise number of assets required in the warehouse to withstand HILP events with various levels of severity.

To address this research gap, this paper proposes a data-driven decision-support framework for emergency resource management in critical infrastructure. By integrating engineering fragility curves

with a unique 10-year operational dataset, our model quantifies the precise number of asset failures required to ensure the rapid restoration of services. The primary contributions of this paper are threefold.

(1) It integrates engineering risk models with real-world asset data to create a scientific tool for strategic resource allocation.

(2) It provides a quantitative model for optimizing crisis warehousing, a key component of emergency logistics, by calibrating fragility curves using historical failure data.

(3) It presents a validated case study using data from the Tehran Regional Electric Distribution Company (TREDC), demonstrating how this technology can be leveraged by emergency managers to enhance resilience, providing a blueprint for other sectors.

Methodology and modeling

To optimize emergency resource management, we propose a framework that integrates engineering fragility models with asset lifecycle dynamics. The modeling process is divided into three key steps: (1) data-driven fragility curve calibration, (2) asset lifetime integration, and (3) spare asset quantification.

As can be seen in Fig. 1, every asset in the normal state has an average failure probability P_λ, but this probability depends on the asset's strength. The failure rate increases with accident severity. After all, the asset will be damaged in a serious accident. To ensure the model reflects reality, we calibrate the fragility curves using the 10-year TREDC operational dataset. By statistically correlating historical asset failure records with meteorological storm intensities, we estimate the failure probability parameters. The failure probability P_F is modeled as a linear function of the disaster parameter (D_P), representing wind speed in this study; see Eq. (1).

The mathematical framework presented in this study is developed on the basis of the first principles of reliability engineering and asset management theory. The linear fragility model (Eqs. 1–6) is adopted as a simplified approximation of hazard susceptibility commonly used in infrastructure risk assessment[18], whereas the dynamic lifecycle matrix derivation (Eqs. 7–20) is an original contribution of this research, formulated to explicitly track assets' aging under network expansion and depreciation rates.

$$P_F = \frac{1-P_\lambda}{F_{Pmax}-F_{Pmin}}(D_P - F_{Pmin}) + P_\lambda \quad (1)$$

where, F_{Pmin} is the wind speed threshold where failures begin, and F_{Pmax} is the wind speed at which total failure is expected.

If we assume that N assets are exposed to the HILP incident, the number of failures is obtained via Eq. (2).

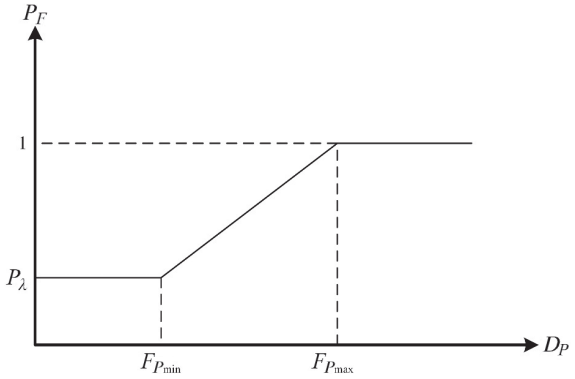

Fig. 1 Conceptual asset fragility curve illustrating failure probability as a function of HILP event severity.

$$N_w^{(D_P)} = \left[\frac{1-P_\lambda}{F_{Pmax}-F_{Pmin}}(D_P - F_{Pmin}) + P_\lambda\right] \times N \quad (2)$$

As the total $N_w^{(D_P)}$ occurs during the HILP period, which is usually a very short time, they should be considered as N_W simultaneous failures. This problem requires a sufficient number of crews, machines, and inventory. Therefore, N_W shows the number of storage required assets. It is observed that the fragility curve is the main data in the N_W calculation and it has different types for different asset lifetimes, in such a way that with an increase in the lifetime of the assets, the severity of the accident F_{Pmin} in which the system totally breaks will be significantly reduced. Therefore, for each lifetime category, a separate fragility curve is considered in Fig. 2.

It is obvious that for each lifetime, $F_{Pmax} >> F_{Pmin}$. Therefore, it is assumed that

$$F_{Pmax}(T_y) > F_{Pmin}(0) \quad (3)$$

As shown in Fig. 2, the slope of the fragility curve is assumed to be the same across different lifetimes. For modeling simplicity and based on a preliminary analysis of the company's failure records, which did not show a statistically significant variation in the failure rate slope across different asset age groups, this assumption was made. Moreover, as the lifetime expectancy increases, the asset's resistance to HILP events decreases, and it is damaged at lower accident intensities. Thus, if the relationship between the severity of the accident at the point of failure (F_P) is plotted in terms of lifetime, Fig. 3 is obtained.

Linearizing F_P and LTF yields Eq. (4).

$$\frac{F_{P0}-F_{PTy}}{0-T_y} = \frac{F_{P0}-F_P}{0-LTF} \Rightarrow F_P(LFT) = F_{P0} - \left(F_{P0}-F_{PT_y}\right)LFT \quad (4)$$

If the number of assets is calculated over different lifetimes, the number of failures is calculated using Eq. (5).

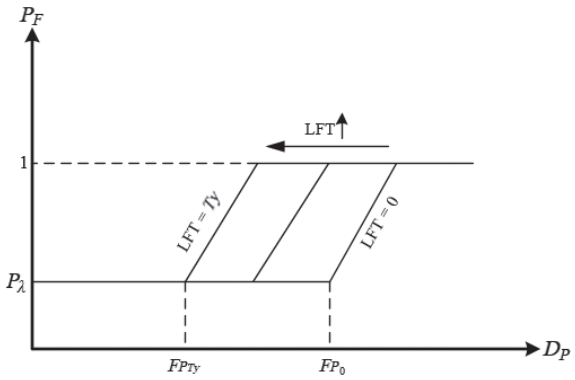

Fig. 2 The impact of asset lifetime on fragility curves, illustrating reduced resilience in older assets.

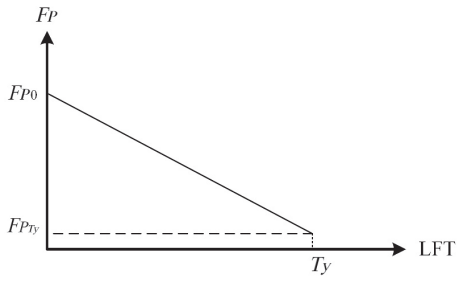

Fig. 3 Linearized relationship between asset lifetime and the failure point (F_P) severity.

$$N_W = \sum P_F(LTF) n_{LTF} \quad (5)$$

P_F The relation P_F (with the help of Fig. 1) is as shown in Eq. (6).

$$P_F(LTF) = \begin{cases} P_\lambda & F_P < F_{P_{min}} \\ \dfrac{1-P_\lambda}{F_{P_{max}} - F_{P_{min}}} F_P(LFT) + P_\lambda & F_{P_{min}} \le F_P \le F_{P_{max}} \\ 1 & F_P < F_{P_{max}} \end{cases} \quad (6)$$

In this way, the flowchart (Fig. 4) for calculating the number of failures and the required spare parts in the warehouse was determined.

NLF is the number of assets in each lifetime, which can be calculated by understanding the development and failure process as follows. If *k* is the base year and *k* = 0 is the base year of the electricity industry, the development process can be plotted in Table 1.

Table 1 is based on equalizing assets (*1 + a*) each year as the distribution network's assets develop. This table shows the number of assets with different lifetimes in year *k* of the electricity industry, assuming that the number of assets at the origin is *N* and the load growth is *a*. In this case, the number of *j*-year assets in the electricity industry in year *K* can be calculated using Eq. (7).

$$n_{kj} = a(1+a)^{k-j-1} \times N \quad (7)$$

$$Assets = \begin{bmatrix} N & 0 \\ (a+\lambda)N & (1-\lambda)N \\ (a+\lambda)(1+a)N & (a+\lambda)(1-\lambda)N \\ \cdots & \cdots \\ (a+\lambda)(1+a)^{m-1}N & (a+\lambda)(1+a)^{m-2}(1-\lambda)N \end{bmatrix}$$

where, *M* is the number of years in the electricity industry from the base year, as can be seen; n_{k_0} is the asset development rate in the year *k*, $\frac{1}{12}$ of which is placed in the monthly warehouse. This matrix has a zero half. The relationships between the rows and columns of the matrix can be written as in Eqs (11) and (12) using Eq. (8):

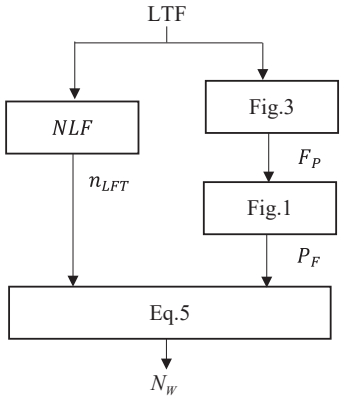

Fig. 4 Flowchart of the proposed model for calculating the required spare assets in the crisis warehouse.

Table 1. Matrix representation of asset count by lifetime (*j*) and year (*k*), considering only annual development.

k	*j*			
	0	1	2	3
0	N			
1	aN	N		
2	$a(1+a)N$	aN	N	
3	$a(1+a)^2N$	$a(1+a)N$	aN	N

However, the depreciation rate of assets is not included in Eq. (7). To consider this parameter, Table 2 is based on the failure rate λ, which is multiplied by the annual assets and rewritten.

Thus, the number of *j*-year assets in year *k* is calculated via Eq. (8).

$$n_{kj} = (a+\lambda)(1+a)^{k-j-1}(1-\lambda)^j N \quad (8)$$

The n_k0 array must be used to find the number of assets required for the development warehouse. Assuming balanced development throughout the year, there are always $\frac{n_{k0}}{12}$ assets in the development warehouse that can be used as a backup for events or in times of crisis. Thus, in the second year of the electricity industry, the development warehouse will have several assets in line with Eq. (9).

$$nY_D = (a+\lambda)(1+a)^{k-1}N = n_{k0} \quad (9)$$

The total available asset is a reliable indicator. Given the load growth rate and failure rate of assets, the number of assets with different lifetimes can be expressed as a simple function of the total number of available assets. For this purpose, based on Eq. (8), a matrix is considered as shown in Eq. (10).

$$\begin{bmatrix} 0 & \cdots & 0 \\ 0 & \cdots & 0 \\ (1-\lambda)^2N & \cdots & 0 \\ \cdots & \cdots & \cdots \\ (a+\lambda)(1+a)^{m-3}(1-\lambda)^2N & \cdots & (1-\lambda)^mN \end{bmatrix} \quad (10)$$

$$\frac{n_{kj}}{n_{(k-1)j}} = 1+a \quad (11)$$

$$\frac{n_{kj}}{n_{k(j-1)}} = \frac{1-\lambda}{1+a} \quad (12)$$

This matrix represents the dynamic lifecycle of assets, accounting for annual load growth (a) and depreciation caused by the failure rate (λ). This allows us to estimate the denominator for Eq. 5.

Equation (11) shows the same relation of n_{kj} with *D* in the relation matrix (10), and Eq. (12) shows the relation n_{kj} with *B* in the relation matrix (10). The sum of each row of the matrix represents the number of assets in year *k*, which is equal to $(1+a)^k N$. Thus, the total number of assets in year *m* can be written as Eq. (13).

$$NOA_m = \sum_{j=1}^{m-1}(a+\lambda)(1+a)^{m-j-1}(1-\lambda)^j N + (1-\lambda)^m N = (1+a)^m N \quad (13)$$

As can be seen from the asset matrix in Eq. (10), each n_{kj} has a row and column relation. For example, in the columnar relation of Fig. 5, Relations 14 and 15 can be written with the help of Eq. (11).

$$n_{(m-1)j} = \frac{n_{mj}}{(1+a)} \quad n_{(m-2)j} = \frac{n_{(m-1)j}}{(1+a)} = \frac{n_{mj}}{(1+a)^2} \quad (14)$$

Table 2. Matrix representation of asset count by lifetime (*j*) and year (*k*) considering both annual development and failure rate (λ).

k	*j*			
	0	1	2	3
0	N			
1	$(a+\lambda)N$	$(1-\lambda)N$		
2	$(a+\lambda)(1+a)N$	$(a+\lambda)(1-\lambda)N$	$(1-\lambda)^2N$	
3	$(a+\lambda)(1+a)^2N$	$(a+\lambda)(1+a)(1-\lambda)N$	$(a+\lambda)(1-\lambda)^2N$	$(1-\lambda)^3N$

Generally, we have

$$\forall j < k < m;\ \ n_{kj} = \frac{n_{mj}}{(1+a)^{m-k}} \tag{15}$$

Equation (15) shows the *j*-year assets in year *k* as a percentage of the *j*-year assets in year *m* for the electricity industry. In this way, the lifetimes of future years' assets are predictable. Figure 6 shows the row relation of the assets matrix. Using Fig. 6 and Eq. (4), Eqs (16)–(19) are obtained.

$$n_{mj} = \frac{1-\lambda}{1+a} n_{m(j-1)} \tag{16}$$

As a result, we have

$$n_{m1} = \frac{1-\lambda}{1+a} n_{m0},\ \ n_{m2} = \frac{1-\lambda}{1+a} n_{m1} = \left(\frac{1-\lambda}{1+a}\right)^2 n_{m0} \tag{17}$$

Generally, the number of assets with different lifetimes related to the development rate of year *m* can be written as shown in Eq. (18):

$$\forall 0 < j \le m:\ n_{mj} = \left(\frac{1-\lambda}{1+a}\right)^j n_{m0} \tag{18}$$

On the other hand, using Eqs (8) and (13), the amount of annual development can be related to the number of available assets, as shown in Eq. (19).

$$\frac{n_{m0}}{NOA_m} = \frac{(\lambda+a)(1+a)^{m-1}N}{(1+a)^m N} = \frac{\lambda+a}{1+a} \tag{19}$$

Using Eq. (19), the number of assets with lifetime *j* can be written as in Eq. (20).

$$n_{mj} = \left(\frac{1-\lambda}{1+a}\right)^j \cdot \frac{\lambda+a}{1+a} . NOA_m \tag{20}$$

Equation (20) shows the number of assets with different lifetimes, which is formulated as the total number of available assets. Thus, the *NLF* relation in Fig. 4 can be represented as shown in Eq. (20). Therefore, N_W can easily be calculated.

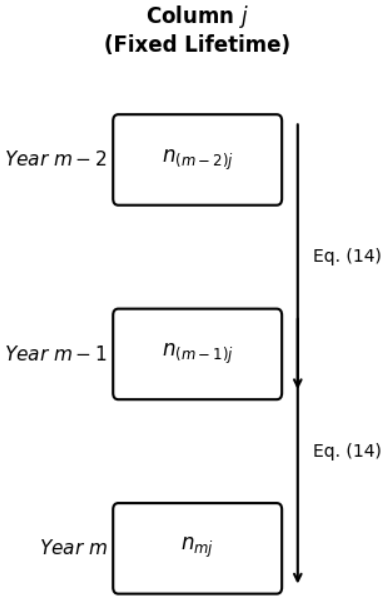

Fig. 5 Schematic of the column-wise relationships within the asset matrix.

$$n_{m0} \quad \ldots \quad n_{m1} \quad n_{m2} \quad \ldots \quad n_{mj} \quad \ldots \quad n_{m(m-1)} \quad \ldots \quad N$$

Fig. 6 Schematic of the row-wise relationships within the asset matrix.

Numerical studies

This study utilizes a comprehensive dataset from TREDC spanning 10 years (2013–2022).

Case study and data description

The dataset contains detailed records of 50,000 distribution transformers and poles. It includes installation dates (for calculating lifetimes), failure logs with timestamps, and maintenance records. Meteorological data, specifically wind speed records, were obtained from the Iran Meteorological Organization. By spatially and temporally matching failure events with storm intensities, we were able to extract the fragility parameters (Dp_{min}, Dp_{max}) for different asset age groups, as detailed in Table 3. According to Eq. (5), the number of assets during different lifetimes is presented in the form of Table 4.

As shown in Table 3, the calibration results confirm that older assets have significantly lower failure thresholds (Dp_{min}, Dp_{max}), validating the degradation model.

As shown in Table 4 and Fig. 7, even at low wind speeds (50–70 km/h), a baseline number of asset failures is predicted. The number of damaged assets, which directly translates to the quantity

Table 3. Extracted fragility parameters (Dp_{min}, Dp_{max}) for assets of varying lifetimes based on TREDC historical data.

LFT	Dp_{min}	Dp_{max}	LFT	Dp_{min}	Dp_{max}
1	120	250	16	90	175
2	118	245	17	88	170
3	116	240	18	86	165
4	114	235	19	84	160
5	112	230	20	82	155
6	110	225	21	80	150
7	108	220	22	78	145
8	106	215	23	76	140
9	104	210	24	74	135
10	102	205	25	72	130
11	100	200	26	70	125
12	98	195	27	68	120
13	96	190	28	66	115
14	94	185	29	64	110
15	92	180	30	62	105

Table 4. Calculated number of damaged assets (N_w), required spare Assets (P_w), and percentage of total assets (*PRC*) at various storm wind speeds (D_p).

DP	N_w	P_w	*PRC*	*DP*	N_w	P_w	*PRC*
50	80.18882	11.53376	0.576688	160	473.0745	68.04348	3.402174
60	80.18882	11.53376	0.576688	170	516.2171	74.24878	3.712439
70	84.36561	12.13452	0.606726	180	555.1179	79.84399	3.992199
80	98.71709	14.19872	0.709936	190	589.6541	84.81142	4.240571
90	123.2898	17.73308	0.886654	200	619.6781	89.12985	4.456492
100	158.6401	22.8176	1.14088	210	645.0183	92.77459	4.63873
110	204.6656	29.43757	1.471878	220	665.479	95.7175	4.785875
120	259.5956	37.33828	1.866914	230	680.8398	97.92688	4.896344
130	319.0274	45.8865	2.294325	240	690.8552	97.92688	4.968371
140	374.4256	53.85456	2.692728	250	695.2532	100	5
150	425.7875	61.24207	3.062103	260	695.2532	100	5

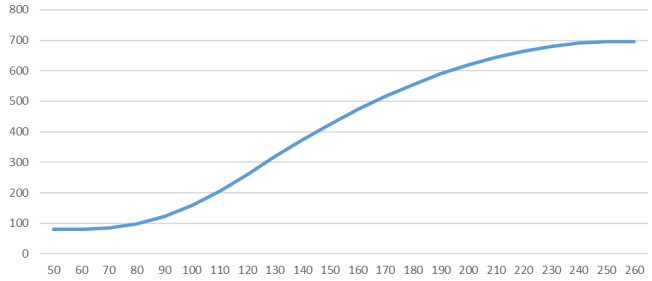

Fig. 7 Estimated number of damaged assets vs. storm wind speed, based on the TREDC dataset.

of spare parts required for storage, increases significantly with higher storm intensities. This quantification allows managers to move from qualitative risk assessment to a data-driven budgeting process for spare parts.

The model's output represents the total number of assets required for the crisis warehouse. However, this quantity can be offset by the assets available in the development warehouse. According to TREDC's operational data, the development warehouse consistently maintains an average of 100 spare assets for routine projects. These assets can be temporarily reallocated during a major HILP event, effectively reducing the required inventory for the crisis warehouse by this amount. Furthermore, the expansion of decentralized generation and mobile emergency units can mitigate the impact of asset failures, though this effect is not quantified in the current model. The relationship between asset growth and the required number of spares is critical. As shown in Table 5 and Fig. 8, a higher asset growth rate (coefficient a) leads to a larger proportion of younger, more resilient assets, which, in turn, reduces the overall number of predicted failures for an event with a given level of severity.

Table 6 and Fig. 9 illustrate the impact of the asset growth rate (a) on the absolute number of damaged assets. A critical insight emerges here: Although a higher growth rate results in a larger proportion of younger, more resilient assets (improving the inventory's average resistance), it also increases the total asset base. Consequently, the absolute number of assets exposed to the hazard rises, leading to a higher number of failures for an event with a given level of severity. This clarifies that network expansion must be accompanied by a proportional scaling of emergency inventory to maintain a constant level of service resilience.

Assets depreciate over time, characterized by the annual failure rate (λ). As expected, a higher failure rate reduces the number of assets surviving to older ages, thereby altering the lifetime distribution. Table 7 and Fig. 10 demonstrate that for a given total asset count, a higher failure rate shifts the population towards newer assets, indirectly reducing the inventory's average age.

The analysis underscores the critical role of asset 'immunization'. For an even with a given intensity, such as a storm with 105 km/h winds, older assets account for a disproportionately high share of total failures (see Fig. 11). Therefore, investing in strengthening or 'immunizing' older assets is a highly effective strategy. This proactive approach reduces the number of assets that would otherwise

Table 5. Sensitivity analysis: Asset count by lifetime for different load growth rates (a) from 0.01 to 0.05.

Number of assets by lifetime	Asset growth rate (a)									
	0.01	%	0.02	%	0.03	%	0.04	%	0.05	%
1	1,000	1	1,000	1	1,000	1	1,000	1	1,000	1
2	980.198	0.980198	970.588	0.970588	961.165	0.961165	951.923	0.951923	942.857	0.942857
3	960.788	0.960788	942.042	0.942042	923.838	0.923838	906.158	0.906158	888.98	0.88898
4	941.763	0.941763	914.334	0.914334	887.961	0.887961	862.592	0.862592	838.181	0.838181
5	923.114	0.923114	887.442	0.887442	853.477	0.853477	821.122	0.821122	790.285	0.790285
6	904.834	0.904834	861.341	0.861341	820.332	0.820332	781.645	0.781645	745.126	0.745126
7	886.917	0.886917	836.007	0.836007	788.475	0.788475	744.065	0.744065	702.547	0.702547
8	869.354	0.869354	811.419	0.811419	757.854	0.757854	708.293	0.708293	662.401	0.662401
9	852.139	0.852139	787.554	0.787554	728.423	0.728423	674.241	0.674241	624.55	0.62455
10	835.265	0.835265	764.39	0.76439	700.135	0.700135	641.825	0.641825	588.861	0.588861
11	818.725	0.818725	741.908	0.741908	672.945	0.672945	610.968	0.610968	555.212	0.555212
12	802.513	0.802513	720.088	0.720088	646.811	0.646811	581.595	0.581595	523.486	0.523486
13	786.622	0.786622	698.908	0.698908	621.693	0.621693	553.633	0.553633	493.572	0.493572
14	771.045	0.771045	678.352	0.678352	597.549	0.597549	527.016	0.527016	465.368	0.465368
15	755.777	0.755777	658.401	0.658401	574.343	0.574343	501.679	0.501679	438.776	0.438776
16	740.811	0.740811	639.036	0.639036	552.039	0.552039	477.56	0.47756	413.703	0.413703
17	726.141	0.726141	620.241	0.620241	530.6	0.5306	454.6	0.4546	390.063	0.390063
18	711.762	0.711762	601.999	0.601999	509.995	0.509995	432.745	0.432745	367.773	0.367773
19	697.668	0.697668	584.293	0.584293	490.189	0.490189	411.94	0.41194	346.758	0.346758
20	683.853	0.683853	567.108	0.567108	471.152	0.471152	392.135	0.392135	326.943	0.326943
21	670.311	0.670311	550.428	0.550428	452.855	0.452855	373.282	0.373282	308.261	0.308261
22	657.038	0.657038	534.239	0.534239	435.269	0.435269	355.336	0.355336	290.646	0.290646
23	644.027	0.644027	518.526	0.518526	418.365	0.418365	338.252	0.338252	274.037	0.274037
24	631.274	0.631274	503.275	0.503275	402.118	0.402118	321.99	0.32199	258.378	0.258378
25	618.774	0.618774	488.473	0.488473	386.502	0.386502	306.51	0.30651	243.614	0.243614
26	606.521	0.606521	474.106	0.474106	371.492	0.371492	291.774	0.291774	229.693	0.229693
27	594.51	0.59451	460.162	0.460162	357.065	0.357065	277.746	0.277746	216.568	0.216568
28	582.738	0.582738	446.628	0.446628	343.198	0.343198	264.393	0.264393	204.192	0.204192
29	571.198	0.571198	433.492	0.433492	329.87	0.32987	251.682	0.251682	192.524	0.192524
30	559.888	0.559888	420.742	0.420742	317.06	0.31706	239.582	0.239582	181.523	0.181523
Total	22,785.6	22.78557	20,115.5	20.11552	17,902.8	17.90277	16,056.3	16.05628	14,504.9	14.50488

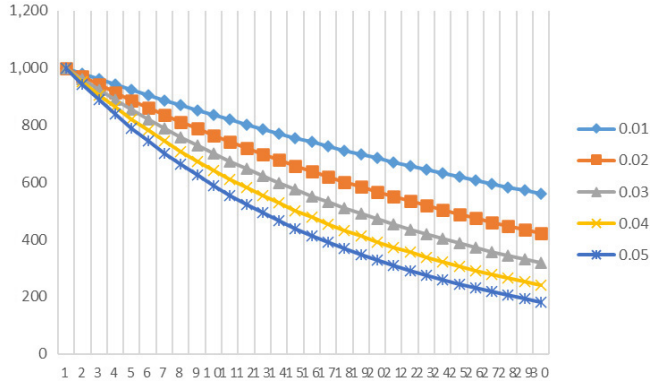

Fig. 8 Distribution of asset count by lifetime for various annual load growth rates (*a*) from 0.01 to 0.05.

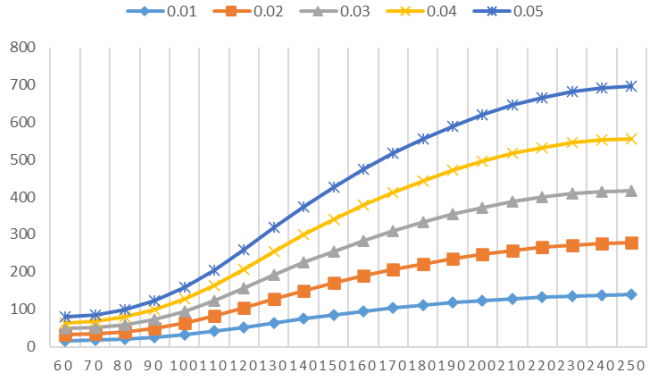

Fig. 9 Impact of asset growth rate (*a*) on the number of damaged assets across various storm severities.

Table 6. Sensitivity analysis: Number of damaged assets at various storm severities for different load growth rates (*a*).

Number of assets damaged in the different accident severities	Asset growth rate (*a*)									
	0.01	%	0.02	%	0.03	%	0.04	%	0.05	%
60	16.04	0.01604	32.08	0.03208	48.11	0.04811	64.15	0.06415	80.2	0.0802
70	16.87	0.01687	33.75	0.03375	50.62	0.05062	67.49	0.06749	84.37	0.08437
80	19.74	0.01974	39.49	0.03949	59.23	0.05923	78.97	0.07897	98.72	0.09872
90	24.66	0.02466	49.32	0.04932	73.97	0.07397	98.63	0.09863	123.29	0.12329
100	31.73	0.03173	63.46	0.06346	95.18	0.09518	126.91	0.12691	158.64	0.15864
110	40.93	0.04093	81.87	0.08187	122.8	0.1228	163.73	0.16373	204.67	0.20467
120	51.92	0.05192	103.84	0.10384	155.76	0.15576	207.68	0.20768	259.6	0.2596
130	63.81	0.06381	127.61	0.12761	191.42	0.19142	255.22	0.25522	319.03	0.31903
140	74.86	0.07486	149.77	0.14977	224.66	0.22466	299.54	0.29954	374.43	0.37443
150	85.16	0.08516	170.31	0.17031	255.47	0.25547	340.63	0.34063	425.79	0.42579
160	94.61	0.09461	189.23	0.18923	283.85	0.28385	378.46	0.37846	473.07	0.47307
170	103.24	0.10324	206.49	0.20649	309.73	0.30973	412.97	0.41297	516.22	0.51622
180	111.02	0.11102	222.05	0.22205	333.07	0.33307	444.09	0.44409	555.12	0.55512
190	117.93	0.11793	235.86	0.23586	353.79	0.35379	471.72	0.47172	589.65	0.58965
200	123.94	0.12394	247.87	0.24787	371.81	0.37181	495.74	0.49574	619.68	0.61968
210	129	0.129	258.01	0.25801	387.01	0.38701	516.01	0.51601	645.02	0.64502
220	133.1	0.1331	266.19	0.26619	399.29	0.39929	532.38	0.53238	665.48	0.66548
230	136.17	0.13617	272.34	0.27234	408.5	0.4085	544.67	0.54467	680.84	0.68084
240	138.17	0.13817	276.34	0.27634	414.51	0.41451	552.684	0.552684	690.86	0.69086
250	139.05	0.13905	278.1	0.2781	417.15	0.41715	556.2	0.5562	695.25	0.69525

fail, thereby decreasing the required inventory for the crisis warehouse and flattening the demand curve for spares.

The model's projection over a five-year horizon (Table 8 and Fig. 12) confirms that with a constant asset growth rate, the absolute number of damaged assets for a given event severity will also increase. This is a direct consequence of a larger asset base, assuming that the failure rate (λ) remains constant. The key insight is that the required size of the crisis warehouse must scale proportionally with the growth of the total asset inventory to maintain a constant level of resilience.

The sensitivity analysis highlights the importance of asset 'immunization' or targeted reinforcement of older infrastructure. Figure 11 confirms that older assets account for a disproportionately high share of total failures. Investing in strengthening these assets effectively raises their fragility thresholds, which flattens the demand curve for spare parts during crises and reduces the required crisis warehouse inventory.

The model's applicability and limitations

Although the proposed framework offers a robust tool for quantifying emergency resource requirements, certain limitations must be acknowledged. First, the model utilizes a linear fragility function (Eq. 1) for computational simplicity. Although validated by the TREDC dataset, nonlinear fragility curves may provide higher precision for specific equipment types or different hazard profiles. Second, the model assumes that the annual failure rate and load growth rate remain constant over the projection horizon. In reality, these parameters can fluctuate because of economic factors or policy changes; thus, the model's projections serve as estimates rather than deterministic predictions. Third, the current framework quantifies the total number of required spares but does not explicitly optimize the spatial distribution of warehouses across the grid, a critical factor for reducing the restoration time. Future work should incorporate geographic information system (GIS) data to optimize the location-based allocation of the crisis inventory alongside the quantity.

Conclusions

This paper presents a data-driven decision-support framework for emergency resource management in power distribution networks. By statistically calibrating engineering fragility curves with a decade

Table 7. Sensitivity analysis: Asset count by lifetime for different failure rates (λ) from 0.01 to 0.05.

Number of assets in each lifetime	λ									
	0.01	%	0.02	%	0.03	%	0.04	%	0.05	%
1	1,000	1	1,000	1	1,000	1	1,000	1	1,000	1
2	961.165	0.961165	951.456	0.951456	941.748	0.941748	932.039	0.932039	922.33	0.92233
3	923.838	0.923838	905.269	0.905269	886.889	0.886889	868.696	0.868696	850.693	0.85069
4	887.961	0.887961	861.324	0.861324	835.225	0.835225	809.659	0.809659	784.62	0.78462
5	853.477	0.853477	819.512	0.819512	786.571	0.786571	754.633	0.754633	723.678	0.72368
6	820.332	0.820332	779.73	0.77973	740.752	0.740752	703.348	0.703348	667.47	0.66747
7	788.475	0.788475	741.879	0.741879	697.601	0.697601	655.547	0.655547	615.628	0.61563
8	757.854	0.757854	705.866	0.705866	656.964	0.656964	610.996	0.610996	567.812	0.56781
9	728.423	0.728423	671.6	0.6716	618.694	0.618694	569.472	0.569472	523.71	0.52371
10	700.135	0.700135	638.998	0.638998	582.654	0.582654	530.77	0.53077	483.034	0.48303
11	672.945	0.672945	607.979	0.607979	548.713	0.548713	494.698	0.494698	445.517	0.44552
12	646.811	0.646811	578.465	0.578465	516.749	0.516749	461.078	0.461078	410.913	0.41091
13	621.693	0.621693	550.385	0.550385	486.647	0.486647	429.742	0.429742	378.998	0.379
14	597.549	0.597549	523.667	0.523667	458.299	0.458299	400.537	0.400537	349.561	0.34956
15	574.343	0.574343	498.246	0.498246	431.602	0.431602	373.316	0.373316	322.411	0.32241
16	552.039	0.552039	474.059	0.474059	406.46	0.40646	347.945	0.347945	297.369	0.29737
17	530.6	0.5306	451.047	0.451047	382.783	0.382783	324.298	0.324298	274.272	0.27427
18	509.995	0.509995	429.151	0.429151	360.485	0.360485	302.258	0.302258	252.97	0.25297
19	490.189	0.490189	408.319	0.408319	339.486	0.339486	281.716	0.281716	233.322	0.23332
20	471.152	0.471152	388.497	0.388497	319.71	0.31971	262.571	0.262571	215.2	0.2152
21	452.855	0.452855	369.638	0.369638	301.086	0.301086	244.726	0.244726	198.485	0.19849
22	435.269	0.435269	351.695	0.351695	283.547	0.283547	228.094	0.228094	183.069	0.18307
23	418.365	0.418365	334.622	0.334622	267.03	0.26703	212.593	0.212593	168.85	0.16885
24	402.118	0.402118	318.378	0.318378	251.474	0.251474	198.145	0.198145	155.735	0.15574
25	386.502	0.386502	302.923	0.302923	236.825	0.236825	184.678	0.184678	143.639	0.14364
26	371.492	0.371492	288.218	0.288218	223.03	0.22303	172.128	0.172128	132.483	0.13248
27	357.065	0.357065	274.227	0.274227	210.038	0.210038	160.43	0.16043	122.193	0.12219
28	343.198	0.343198	260.915	0.260915	197.803	0.197803	149.527	0.149527	112.702	0.1127
29	329.87	0.32987	248.249	0.248249	186.28	0.18628	139.365	0.139365	103.949	0.10395
30	317.06	0.31706	236.198	0.236198	175.429	0.175429	129.893	0.129893	95.8749	0.09587
	17,902.8	17.90277	15,970.5	15.97051	14,330.6	14.33057	12,932.9	12.93289	11,736.5	11.7365

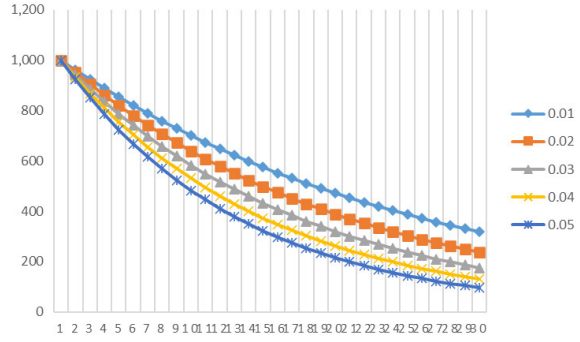

Fig. 10 Sensitivity of asset lifetime distribution to variations in the annual failure rate (λ).

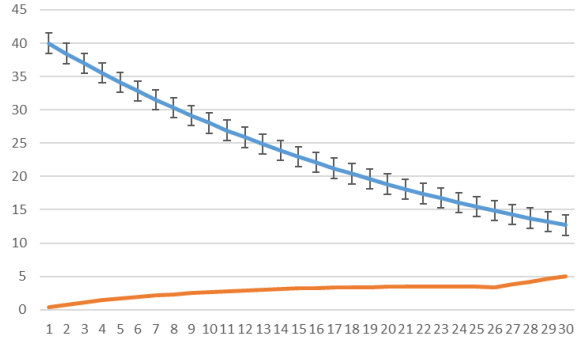

Fig. 11 Distribution of available vs. damaged assets by lifetime at a specific storm severity (105 km/h).

of operational data from TREDC, we transformed the qualitative process of crisis warehousing into a quantitative, scientifically grounded practice. The results demonstrate that spare asset

Table 8. Projection of potential failures over 5 years at a storm severity of 110 km/h and a 3% asset growth rate.

Severity	Total number of assets				
	20,000	20,600	21,218	21,854.5	22,510.2
60	80.2	82.606	85.0842	87.6367	90.2658
70	84.37	86.9011	89.5081	92.1934	94.9592
80	98.72	101.682	104.732	107.874	111.11
90	123.29	126.989	130.798	134.722	138.764
100	158.64	163.399	168.301	173.35	178.551
110	204.67	210.81	217.134	223.648	230.358
120	259.6	267.388	275.41	283.672	292.182
130	319.03	328.601	338.459	348.613	359.071
140	374.43	385.663	397.233	409.15	421.424
150	425.79	438.564	451.721	465.272	479.23
160	473.07	487.262	501.88	516.936	532.445
170	516.22	531.707	547.658	564.088	581.01
180	555.12	571.774	588.927	606.595	624.793
190	589.65	607.34	625.56	644.327	663.656
200	619.68	638.27	657.419	677.141	697.455
210	645.02	664.371	684.302	704.831	725.976
220	665.48	685.444	706.008	727.188	749.004
230	680.84	701.265	722.303	743.972	766.291
240	690.86	711.586	732.933	754.921	777.569
250	695.25	716.108	737.591	759.718	782.51

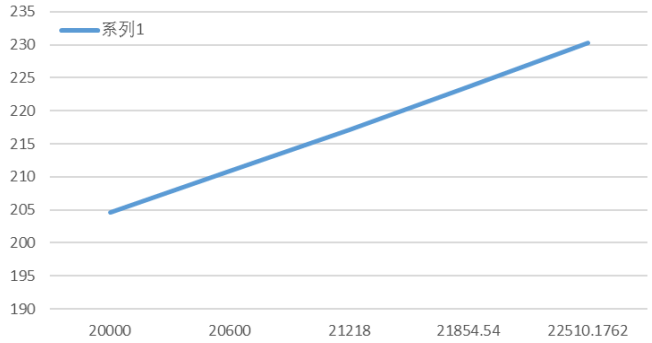

Fig. 12 Projection of potential asset failures over five consecutive years at a storm severity of 110 km/h, assuming a 3% annual asset growth rate.

requirements are highly sensitive to storms' severity, assets' age distribution, and the network's growth rates. Specifically, we clarified that although network growth improves the average age of assets, it increases the absolute number of assets at risk, requiring larger emergency inventories. This framework provides utility managers with a powerful tool to optimize resource allocation, ensuring that resilience planning keeps pace with infrastructure expansion and climate challenges. Future research will focus on integrating an optimization layer to minimize the total cost (inventory holding cost + shortage penalty) and exploring the impact of decentralized generation and mobile emergency units on reducing dependence on warehouses.

Author contributions

The authors confirm their contribution to the paper as follows: Validation, resources, methodology, software, formal analysis, investigation, writing – original draft: Yousefi Jooben A; conceptualization, supervision, writing – review and editing: Dashti R. All authors reviewed the results and approved the final version of the manuscript.

Data availability

The datasets generated during and/or analyzed in the current study are available from the corresponding author on reasonable request. The data are not publicly available because of privacy/ethical restrictions associated with the operational records of TREDC.

Acknowledgments

This work was supported by the Iran University of Science and Technology. We acknowledge TREDC for providing the operational data used in this study.

Conflict of interest

The authors declare that they have no conflict of interest.

Dates

Received 13 December 2025; Revised 19 February 2026; Accepted 16 March 2026; Published online 25 May 2026

References

[1] Kessides IN. 2013. Chaos in power: Pakistan's electricity crisis. *Energy Policy* 55:271–285

[2] Rasoulkhani K, Mostafavi A, Cole J, Sharvelle S. 2019. Resilience-based infrastructure planning and asset management: study of dual and singular water distribution infrastructure performance using a simulation approach. *Sustainable Cities and Society* 48:101577

[3] Rachunok B, Nateghi R. 2020. The sensitivity of electric power infrastructure resilience to the spatial distribution of disaster impacts. *Reliability Engineering & System Safety* 193:106658

[4] Wan S. 2017. Asset performance management for power grids. *Energy Procedia* 143:611–616

[5] Argyroudis SA, Mitoulis SA, Hofer L, Zanini MA, Tubaldi E, et al. 2020. Resilience assessment framework for critical infrastructure in a multi-hazard environment: case study on transport assets. *Science of the Total Environment* 714:136854

[6] Waseem M, Manshadi SD. 2020. Electricity grid resilience amid various natural disasters: challenges and solutions. *The Electricity Journal* 33:106864

[7] Chung SY, Xu Y. 2020. Reliability and resilience in a regulated electricity market: Hong Kong under Typhoon Mangkhut. *Utilities Policy* 67:101134

[8] Kelly-Gorham MR, Hines PDH, Zhou K, Dobson I. 2020. Using utility outage statistics to quantify improvements in bulk power system resilience. *Electric Power Systems Research* 189:106676

[9] Mirzaei MJ, Dashti R, Kazemi A, Amirioun MH.2015. An asset-management model for use in the evaluation and regulation of public-lighting systems. *Utilities Policy*. 32:19–28

[10] Fenrick SA, Getachew L. 2012. Cost and reliability comparisons of underground and overhead power lines. *Utilities Policy* 20(1):31–37

[11] Catrinu MD, Nordgård DE. 2011. Integrating risk analysis and multi-criteria decision support under uncertainty in electricity distribution system asset management. *Reliability Engineering & System Safety* 96(6):663–670

[12] Ouyang M, Wang Z. 2015. Resilience assessment of interdependent infrastructure systems: with a focus on joint restoration modeling and analysis. *Reliability Engineering & System Safety* 141:74–82

[13] Home-Ortiz JM, Yamaguti LC, Yumbla J, Melgar-Dominguez OD, Machado Monaro R, et al. 2025. Resilience-oriented planning for distribution systems combining distributed generation allocation and dynamic operational strategies. *IEEE Access* 13:154556–154567

[14] Ma S, Chen B, Wang Z. 2018. Resilience enhancement strategy for distribution systems under extreme weather events. *IEEE Transactions on Smart Grid* 9(2):1442–1451

[15] Yuan W, Wang J, Qiu F, Chen C, Kang C, et al. 2016. Robust optimization-based resilient distribution network planning against natural disasters. *IEEE Transactions on Smart Grid* 7(6):2817–2826

[16] Kwasinski A, Weaver WW, Chapman PL, Krein PT. 2009. Telecommunications power plant damage assessment for hurricane katrina– site survey and follow-up results. *IEEE Systems Journal* 3(3):277–287

[17] Joobeni AY, Naghavi M, Dashti R. 2026. Economic sustainability of urban power distribution asset management: a framework for stability planning in metropolitan grids. *Results in Engineering* 29:108583

[18] Modarres M, Kaminskiy MP, Krivtsov V. 2016. *Reliability Engineering and Risk Analysis: A Practical Guide*. 3rd Edition. Boca Raton: CRC Press. doi: 10.1201/9781315382425